Ceramics International xxx (xxxx) xxx–xxx

Contents lists available at ScienceDirect

Ceramics International

journal homepage: www.elsevier.com/locate/ceramint

The dielectric, thermal properties and crystallization mechanism of Li–Al – B–Si – O glass – Ceramic systems as a new ULTCC material

Guanyu Chen[a,b,c], Mingsheng Ma[a], Anqing Wei[a,b], Zhifu Liu[a,b,**], Faqiang Zhang[a], Arnan Mitchell[c], Yongxiang Li[a,c,*]

[a] CAS Key Lab of Inorganic Functional Materials and Devices, Shanghai Institute of Ceramics, Chinese Academy of Sciences, Shanghai, 200050, China
[b] Center of Materials Science and Optoelectronics Engineering, University of Chinese Academy of Sciences, Beijing, 100049, China
[c] School of Engineering, RMIT University, Melbourne, Victoria, 3000, Australia

ARTICLE INFO

Keywords:
LABS glass-ceramic
ULTCC
Dielectric property
CTE
Crystallization kinetic
Base metallization

ABSTRACT

Li–Al–B–Si–O (LABS) glass-ceramics with a sintering temperature of 600 °C were studied for ultra-low temperature co-fired ceramics (ULTCC) applications. The crystal phase of LABS glass-ceramics is dendritic β-spodumene. The permittivity and dielectric loss of LABS glass-ceramics are $\varepsilon_r = 5.8$ and $tg\delta = 1.3 \times 10^{-3}$ at 10 MHz, respectively. The coefficient of thermal expansion (CTE) of LABS glass-ceramics is 3.23 ppm/°C, which is close to that of silicon. The dielectric and thermal properties of LABS glass-ceramics are closely correlated to the degree of its crystallization. The permittivity decreases continually while the dielectric loss decreases first and slightly increases with the increasing of crystallization of β-spodumene. The CTE of LABS glass-ceramics decreases as β-spodumene crystallized from LABS glass. The crystallization kinetic and mechanism of LABS glass-ceramics indicate that the β-spodumene crystallizes in a two-dimensional interfacial growth mechanism due to the migration of Li-ions. The diffusion coefficients derived from energy-dispersive X-ray spectroscopy (EDS) results indicated that both Al and Ag electrodes have good compatibilities with ULTCC tapes, which could reduce the cost of multilayer electro-ceramic devices dramatically by using the ULTCC and base metallization.

1. Introduction

The multilayer ceramic structures with embedded electrode lines and vias by low temperature co-fired ceramics (LTCC) technology provide unique advantages in miniaturization and high density packaging of electronic systems [1]. In the past decades, LTCC technology has made great progresses as a plentiful of materials such as Al_2O_3 system, TiO_2 system, $BaO–TiO_2$ system, columbite, ABO_3 (A = Mg, Ca, Zn; B = Ti) system, Bi_2O_3-based compounds, and Li-based compounds have been widely developed, vastly expanding its applications in high quality microelectronic devices [2]. Recently, ultra-low temperature co-fired ceramics (ULTCC) technology, which are sintered under 650 °C, has attracted increasing attentions for the next generation of low-cost LTCC products such as filters and substrates [3,4]. The low sintering temperature not only enables LTCC to co-fire with low melting point metal electrodes such as Al, which are vastly used in semiconductor industry due to its low cost, but also brings LTCC the benefits of packaging with silicon based IC devices or plastics [5]. These merits could pave the avenue to the cutting-edge of ULTCC, which is becoming the next generation LTCC technology [6–9].

Generally, ULTCC requires low permittivity and low dielectric loss for GHz wireless communications, and the ability to integrate with passive components such as resonators, inductors, resistors and capacitors to fabricate integrated circuits (ICs). In addition, it also demands a silicon matched CTE for silicon-based devices packaging [5,9]. Many studies of ULTCC materials focus on molybdate, tellurate and vanadate systems due to their intrinsic low sintering temperatures. These systems have permittivities in the range of 4.1–81, Q × f in the range of 5000–43000 GHz, and mostly belong to glass-free systems [10–13]. Recently, some glass-based systems, which are analogous to the commercialized LTCC material systems, have been investigated as well. Yu et al. studied the Zn–B–O (ZB) glass-ceramics and ZB-glass + SiO_2 system, which both exhibited good dielectric properties. The permittivity of ZB glass-ceramics was 7.5 and dielectric loss was 6×10^{-4} at

* Corresponding author. CAS Key Lab of Inorganic Functional Materials and Devices, Shanghai Institute of Ceramics, Chinese Academy of Sciences, Shanghai, 200050, China.
** Corresponding author. CAS Key Lab of Inorganic Functional Materials and Devices, Shanghai Institute of Ceramics, Chinese Academy of Sciences, Shanghai, 200050, China.
E-mail addresses: liuzf@mail.sic.ac.cn (Z. Liu), yxli@mail.sic.ac.cn (Y. Li).

https://doi.org/10.1016/j.ceramint.2019.06.220
Received 1 May 2019; Received in revised form 5 June 2019; Accepted 20 June 2019

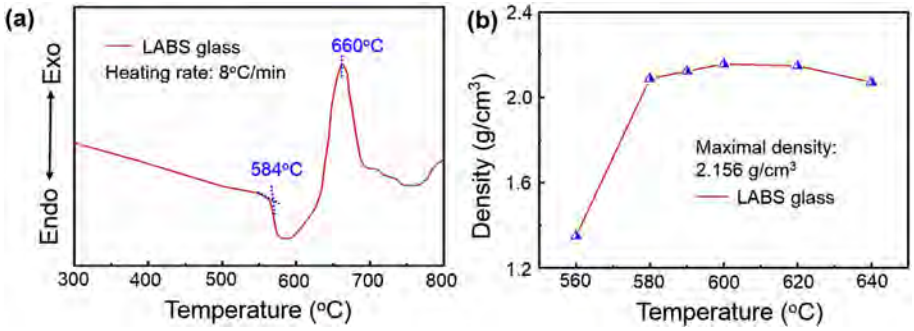

Fig. 1. (a) The DTA curve with a heating rate of 8 °C/min of LABS glass, (b) The densities of LABS glass-ceramics as a function of sintering temperature.

10 MHz, while ZB glass + SiO_2 system showed a permittivity of 6.1 and a dielectric loss of 1.3×10^{-3} at 1 MHz [14,15]. Ma et al. studied the Cu–B–Li–O (CBL) glass-ceramics which showed excellent microwave dielectric properties with $\varepsilon_r = 5.84$, $Q \times f = 10120$ GHz (at 13.44 GHz), and $\tau_f = -33$ ppm/°C [16]. In glass based systems, the dielectric properties are determined by its crystal phase, glass phase and their proportions. Apart from dielectric properties, the CTE of glass-based systems, which is critical for packaging, is also determined by its phases and their proportions. Therefore, in order to obtain good dielectric and thermal properties, it is important to study the crystallization mechanism of glass-based ULTCC materials. As for packaging with passive components, the chemical compatibility of dielectrics and metal electrodes is critical, which is commonly investigated by co-firing with Al or Ag pastes. However, to date, only few studies have reported the compatibility of dielectrics with Al paste.

The Li_2O–Al_2O_3–SiO_2 (LAS) system has been extensively used in aerospace fields for their low, zero or even negative CTE, excellent thermal shock resistant properties and high chemical durability [17]. Besides, the LAS system also shows excellent microwave dielectric properties. Kweon et al. reported that the LAS ceramics containing 12.0 mol% of B_2O_3 exhibited the microwave dielectric properties of $\varepsilon_r = 5.3$, $Q \times f = 212000$ GHz and $\tau_f = -7.7$ ppm/°C. The addition of B_2O_3 also decreased sintering temperature of LAS ceramics down to 950 °C by forming a liquid phase with Li_2O [18]. However, the sintering temperature is still too high for ULTCC applications.

In this work, we developed a new kind of glass-based ULTCC material, Li–Al–B–Si–O (LABS) glass-ceramic. The relation of dielectric, thermal properties and crystallization kinetics were systematically studied. The dielectric properties, CTE of LABS glass-ceramics and their co-sinterability with Al and Ag electrodes were investigated.

2. Experiment procedure

The LABS glass consisted of 15 wt% Li_2CO_3, 20 wt% Al_2O_3, 15 wt% B_2O_3, 50 wt% SiO_2 were prepared by traditional melt method, and then wet-milled into glass powders with a diameter of 1 μm. The LABS glass powders were mixed with 8% polyvinyl alcohol (PVA), pressed into disks (Φ13 mm × 1 mm) and bars (5 mm × 5 mm × 30 mm) under a uniaxial pressure of 2 MPa. After de-bindered at 450 °C, the disks and bars were sintered at different temperatures (from 560 °C to 640 °C) and times (for 20–360 min). The bar samples (4 mm × 4 mm × 25 mm) were prepared for CTE measurement. A slurry by mixing the glass powders with solvent, plasticizers, a binder and a dispersant for 24 h was prepared and tape cast for LTCC green-tapes. The solvent was a mixture of ethanol and ethyl-acetate (1:1 mass ratio). The plasticizers were polyethylene-400 (PEG-400) and butyl-benzyl-phthalate (BBP) (1:1 mass ratio). The binder was poly vinyl-butyral (PVB) and the dispersant was glyceryl. The ratio of solvent, plasticizers, a binder and a dispersant was 20:2:4:1. The details about the fabrication of green tapes can be found in our previous work [19]. Al (PV3Nx) and Ag (LL612, DuPont, USA) electrode pastes were screen printed on the surface of green tapes. The green tapes were stacked and hot isostatic laminated at 65 °C and 50 MPa for 15 min. The samples were de-bindered at 450 °C and the laminated modules were sintered at 600 °C for 70 min in a reducing atmosphere (H_2 and N_2).

Differential thermal analysis (DTA, 404 PC, Netzsch, Germany) was applied at heating rates from 4 to 20 °C/min in a flowing air. The bulk density of sintered LABS glass-ceramics was measured using Archimedes method. The crystalline phase of sintered LABS glass-ceramics were identified by X-ray diffraction (XRD, D8 Advance, Bruker, Germany). The microstructures of sintered LABS glass-ceramics were identified by scanning electron microscope (SEM, XL30, Phillips, The Netherlands) while energy-dispersive X-ray spectroscopy was employed for elemental analysis (EDS, X-MaxN80, Oxford, UK). The thermal expansion coefficient was determined using a dilatometer (DIL, 402C, Netzsch, Germany) from 25 to 300 °C at a heating rate of 10 °C/min in air.

3. Results and discussion

Fig. 1a shows the DTA curve of LABS glass powder with a heating rate of 8 °C/min from 300 °C to 800 °C. It can be seen that the glass transition temperature (T_g) and crystallization temperature (T_c) are 584 °C and 660 °C, respectively. The densities of sintered samples are shown in Fig. 1b, which increase from 560 °C to 600 °C and decrease from 600 °C to 640 °C. The optimal sintering temperature is 600 °C, which belongs to ULTCC [20]. The SEM images of samples sintered for 20 min at different temperatures are shown in Fig. 2. As sintering temperature increases, the samples become dense and pores almost disappear at 600 °C because of the glass transition, which is consistent with DTA results. With a further increase of the sintering temperature, the glass starts to crystalize and pores form which result in a slightly decrease of density. The gray areas, dark regions and light dots can be observed in SEM images. The gray areas are grains and appears when

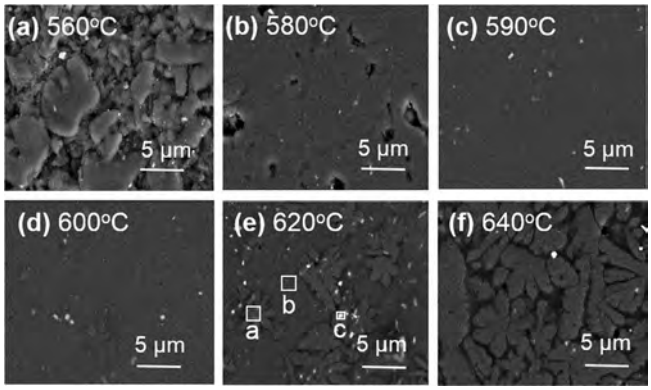

Fig. 2. SEM images of LABS glass-ceramics sintered for 20 min at different temperatures: (a) 560 °C, (b) 580 °C, (c) 590 °C, (d) 600 °C, (e) 620 °C and (f) 640 °C.

Table 1
The EDS results of atomic percent of Al, Si, O and Zr elements at different areas.

Areas	Al (atomic percent)	O (atomic percent)	Si (atomic percent)	Zr (atomic percent)
a	8.37	16.79	74.84	0
b	6.91	14.79	78.3	0
c	0.59	0.64	77.12	21.66

the sintering temperature is above 600 °C, which corresponds to the crystallization temperature in DTA curve. The atomic ratio of different elements, which are derived from EDS results of three areas, are listed in Table 1. As light elements, lithium (Li) and boron (B) cannot be detected via EDS. The elements of Al, Si and O are detected in areas (a) and (b). However, area (c), where is the light dots, almost exclusively contains Zr and O. The light dots are evenly dispersed in the sintered samples from the SEM images (a to f), indicating they may come from the ball mill process, where zirconia balls are used. The atomic ratios of Al and Si in area (a) and area (b) are close to 1:2. The grains are dendritic and the size of grains increase from 3 μm to 10 μm, indicating the crystallization of LABS glass increase. The crystallization of grains also increases as increasing the sintering time at a certain temperature.

Fig. 3 shows the XRD results of samples sintered at 600 °C for different soaking times ranging from 20 to 360 min. The crystal phase is β-spodumene (ICDD file card no. 35–0797) and ZrO_2 (ICDD file card no. 50–1089) is detected, which is correspond to the EDS result. The crystal phase is identical and the intensities enhance as increasing the soaking time, indicating the increase of crystallization of β-spodumene. Fig. 4 represents the dielectric properties (at 10 MHz) of LABS glass-ceramics sintered at 600 °C for different soaking times from 20 to 360 min. The permittivity decreases with increasing soaking time. As shown in Figs. 3 and 7, the proportion of β-spodumene increases when prolong the soaking time, which results in the decrease of permittivity [17]. However, the dielectric loss decreases and increases slightly as prolonging the soaking time. The glass phase usually has high dielectric loss, thus reduces the dielectric loss as increasing soaking time [21]. The prolonging of soaking time also brings the reappearance of pores which lead to extrinsic dielectric loss. The LABS glass-ceramics sintered at 600 °C for 100 min exhibits a permittivity of 5.8 and a dielectric loss of 1.3×10^{-3} at 10 MHz, which can be utilized as an advanced ULTCC substrate material. In order to package with Si based devices, the CTE of LABS is required to match with that of silicon (3.2 ppm/°C, 25–300 °C). The experiment values derived from CTE test are shown in Fig. 5. The results suggest that the CTE of LABS glass-ceramics can be tailored by

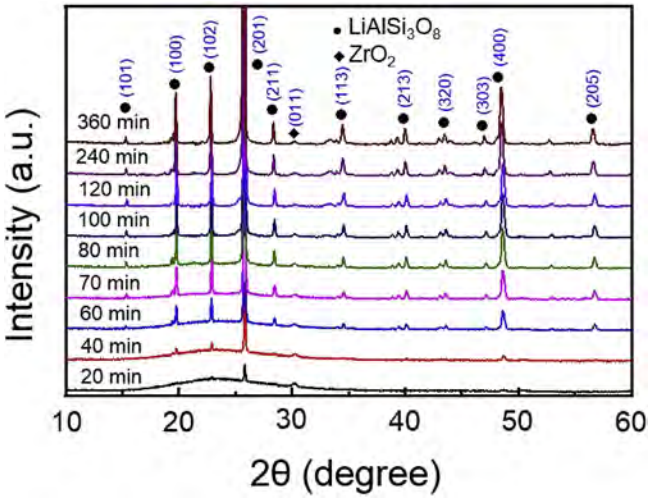

Fig. 3. XRD patterns of LABS glass-ceramics sintered at 600 °C from 20 to 360 min.

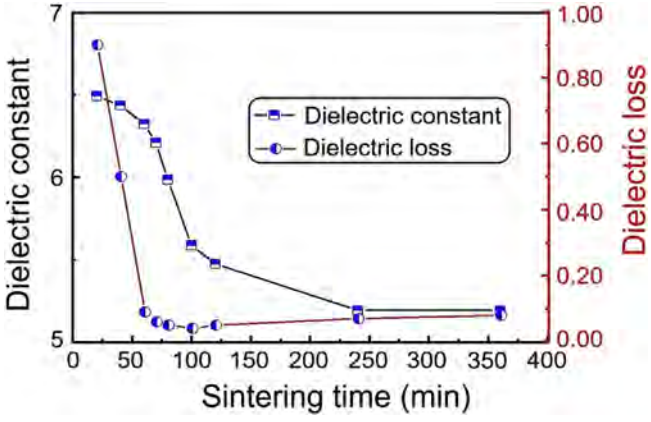

Fig. 4. Dielectric properties (at 10 MHz) of LABS glass-ceramics sintered at 600 °C as a function of sintering time.

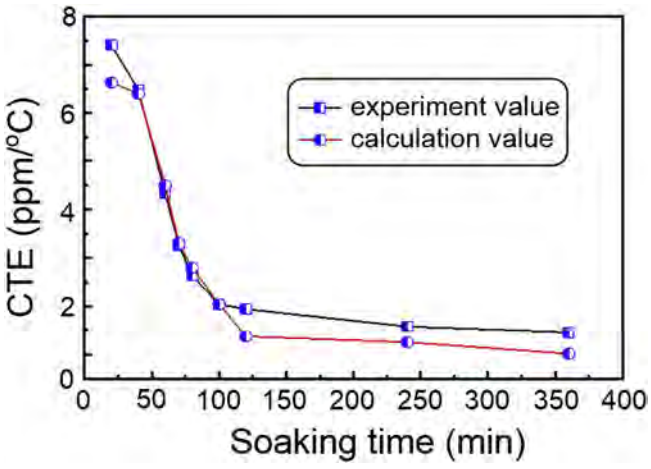

Fig. 5. CTE results of LABS glass-ceramics sintered at 600 °C as a function of sintering time.

the crystallization time during the sintering process. As increasing the soaking time, the CTE values decrease from 6.63 ppm/°C to 1.02 ppm/°C. When sintering at 600 °C for 70 min, the CTE of sample is 3.23 ppm/°C, which matches to that of silicon. The β-spodumene has low CTE due to its special spiral chain-type microstructure [17]. However, the CTE of LABS glass-ceramics sintered at 600 °C for 20 min is 6.63 ppm/°C. It could be attributed to the glass phase. When increase the soaking time, the CTE of samples decreases because of the crystallization of β-spodumene. As same as the dielectric properties of LABS glass-ceramics, the CTE of LABS glass-ceramics mainly depends on the volume fractions of crystal and glass phases [22]. Therefore, it is significant to study the crystallization behavior of LABS glass.

Fig. 6 shows the microstructure of samples sintered at 600 °C with different soaking times from 20 to 360 min. The numbers of β-spodumene grains are measured by using image analyzer in per unit area. The number densities of β-spodumene grains are invariable for samples for the soaking time from 60 to 360 min, indicating the crystallization behavior is a heterogeneous nucleation process, which is a zero-nucleation rate. The areas ratio of grains to the entire figures are calculated and shown in Fig. 7a, serving as an indicator of the volume fraction of β-spodumene. The sigmoidal curve finally shows a plateau as the soaking time increased. The results are analyzed further to the study of the crystallization mechanism using the equation by Avrami and Ozawa as follows [23–26],

$$\ln\{\ln[1/(1-Y)]\} = n\ln k + n\ln t \quad (1)$$

Where, Y is the fraction of precipitated β-spodumene at a time t, n is the

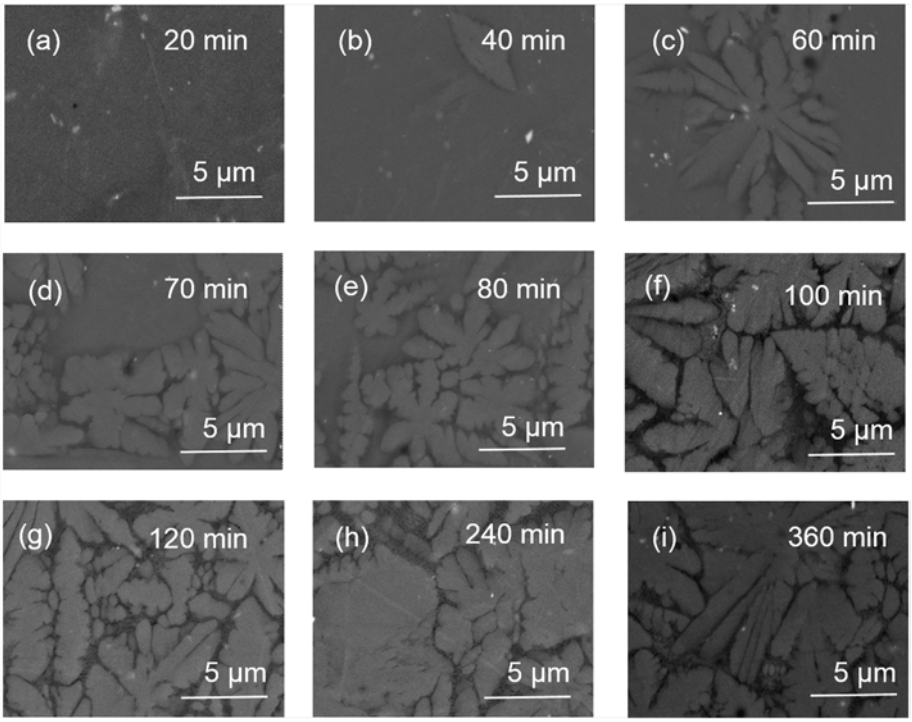

Fig. 6. SEM images of Li–Al–B–Si–O glass sintered at 600 °C as a function of time (a) 20 min, (b) 40 min, (c) 60 min (d) 70 min, (e) 80 min, (f) 90 min, (g) 120 min, (h) 240 min and (i) 360 min.

Avrami exponent, and k is a crystalline rate constant. The Avrami exponent n is determined by plotting $\ln\{\ln[1/(1-Y)]\}$ *vs* $\ln t$. The calculated n is 2.17 from Fig. 7b. The possible n values, which determines the mechanism of crystallization behavior, are listed in Table 2. The calculated value is close to 2, indicating the crystallization of β-spodumene is a two-dimensional interfacial growth ($n = 2$). The intensities of XRD patterns in Fig. 3 are also employed to study the crystallinity of glass-ceramics according to the equation derived by Ohlberg and Strickler as follows [27,28],

$$Y = 100\%(I_g\text{-}I_x)/(I_g\text{-}I_B) \quad (2)$$

Where, Y is the fraction of precipitated β-spodumene in glass, I_g, I_x and I_B are the intensities of parent glass, partly crystalized glass and the mechanical mixture of crystalline compounds respectively at the same value 2θ. The calculation values of crystallinity are also shown in Fig. 7a. Similarly, the curve is a sigmoidal curve. The volume fractions of β-spodumene are close to the results derived from SEM except samples sintered at 600 °C for 20 min and 40 min. By using Eq (3), the Avrami exponent n obtained by plotting $\ln\{\ln[1/(1-Y)]\}$ vs $\ln t$ is 2.27 as shown in Fig. 7b. The similar Avrami exponent n once again identifies the crystallization of β-spodumene, as a two-dimensional interfacial growth. The crystallization mechanism and kinetics of LABS glass-ceramics control its growth process, which determine its dielectric and thermal properties. The CTE of β-spodumene is near zero. According to the experiment results, the CTE of glass phase is approximately 6.63 ppm/°C. Usually, the CTE of glass ceramics is calculated by the following equation [22,29]:

$$\alpha = \sum \chi_i \alpha_i \quad (3)$$

where, α is the CTE of glass-ceramics, χ_i and $\alpha_i$are the volume fraction (χ_i from SEM results) and CTE value of crystal phase and glass. The

Table 2
Theoretical Values and Calculation Values from XRD Results and SEM Results of Avrami Exponent, n, at Zero Nucleation Rate.

	Diffusion-controlling	Reaction-controlling
3-dimension	1.5	3
2-dimension	1	2
1-dimension	0.5	1
n (from XRD)	2.27	
n (from SEM)	2.17	

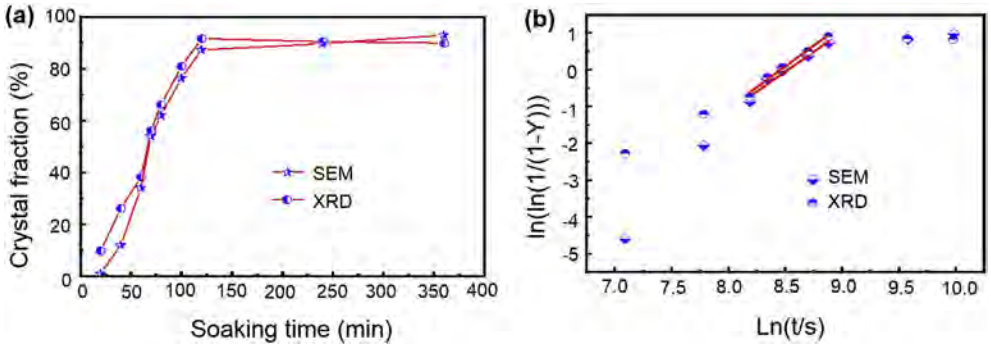

Fig. 7. (a) Crystalline fraction of LABS glass-ceramics derived from SEM and XRD, (b) Avrami plots of $\ln\{\ln[1/(1-Y)]\}$ *vs* $\ln t$ at 600 °C.

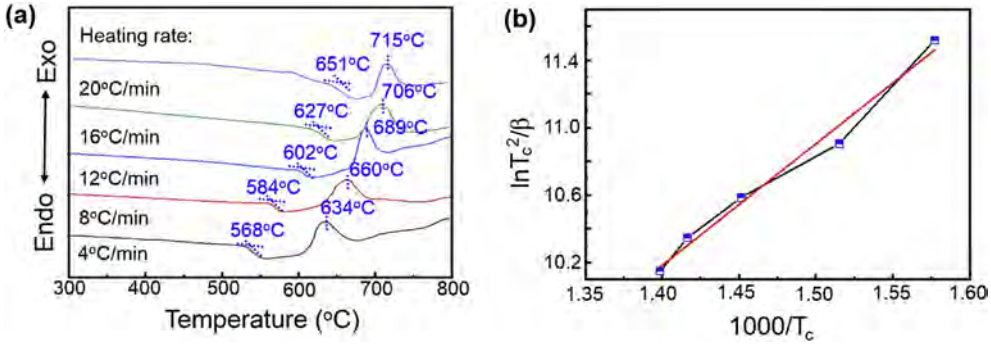

Fig. 8. (a) DTA results of LABS glass at different heating rates from 4 to 20 °C/min, (b) The relationship between $\ln(T_c^2/\beta)$ and $1000/T_c$ for LABS glass.

calculated CTE values of LABS glass-ceramics are shown in Fig. 5 by using Eq (3). It can be observed that the calculation results are close to the experiment results for samples sintered at 600 °C for 40–100 min. The dielectric and thermal properties of LABS glass are determined by its crystallization process. Therefore, in order to tailor its dielectric and thermal properties, the study of its crystallization kinetics is necessary.

Fig. 8a shows the DTA curves for glass powders at the heating rates ranging from 4 to 20 °C/min. One T_c peak and one T_g are observed in each curve. It can be seen that the T_g and T_c shift to higher temperatures with increasing heating rates due to the heat transfer. The DTA results are further analyzed by employing the Kissinger equation proposed by Matusita and co-workers as follows [30]:

$$\ln(T_c 2/\beta)\frac{E}{RT_c} + C \tag{4}$$

where, β is the heating rate, E is the activation energy of crystallization, R is the gas constant, and C is a constant. From Eq (4), the activation energy E, which is determined from the slop in Fig. 8b, is 59.9 kJ/mol. Compared to the different bond energy in glass, it is close to the bond energy of Li–O (ranging from 67.5 to 92 kJ/mol) in glass system [31,32]. Therefore, the crystallization kinetic of LABS glass is determined by the diffusion of Li-ions.

Compared to co-firing with Al metal powders, the embedded Al electrodes are more feasible for ULTCC applications [15,16]. The embedded Al and Ag electrodes are fabricated by screen printing and the concentration profiles of them are shown in Fig. 9. The inserts are the cross-sections of sintered LABS glass-ceramics and embedded electrodes. The SEM images show dense microstructures and no cracks or diffusion at the interfaces, which proves good chemical compatibility of both Al and Ag electrodes. The concentration of embedded aluminum and silver are calculated to study the co-firing process [33]:

$$C_{Al,Ag}(x, t)/C_{Al,Ag} = 1 - erf\,[x/2\sqrt{D_{Al,Ag}\,t}\,] \tag{5}$$

where, $C_{(Al,\ Ag)}$ equals to 100% for aluminum or silver, $C_{(Al,\ Ag)}(x, t)$ is the concentration of aluminum or silver measured at distance x from the interface for sintering time t, D is the diffusion coefficient of Ag or Ag, and the erf is error function. The ratio of $C_{(Al,\ Ag)}(x, t)/C_{(Al,\ Ag)}$ was obtained from EDS results. The diffusion coefficient of aluminum in ULTCC determined by Eq. (5) is 3.3×10^{-14} cm [2]/s at 600 °C, while the diffusion coefficient of silver is 8.9×10^{-14} cm [2]/s at 600 °C. These values are lower than previously reported results which used CuO to suppress the silver diffusion in LTCC [33,34]. According to the images of cross-section and the calculation results, the aluminum and silver electrodes both have good compatibilities with the ULTCC tapes.

4. Conclusions

A Li–Al–B–Si–O (LABS) glass-ceramic system with a sintering of 600 °C was studied for ULTCC applications. The permittivity and dielectric loss of LABS glass-ceramics are 5.8 and 1.3×10^{-3} at 10 MHz. The CTE of the LABS glass-ceramic can be tailored to be 3.23 ppm/°C, which is close to that of silicon. The dielectric and thermal properties of LABS glass-ceramics are correlated to its crystallization behavior. The activation energy calculated from DTA data is 59.9 kJ/mol, suggesting LABS glass has a low crystallization temperature. The XRD and SEM results identify that the crystal phase is dendritic β-spodumene. The Avrami exponent calculated from XRD and SEM results indicates that β-spodumene grows up in a two-dimensional interfacial growth mechanism. The diffusion coefficients derived from EDS results indicated that the aluminum and silver electrodes both have good compatibilities with the LABS ULTCC tapes, which could reduce the cost of multilayer ceramic devices and systems significantly for the future applications.

Acknowledgments

The authors would like to acknowledge the financial support from the National Key Research and Development Program of China (2017YFB0406303), National Natural Science Foundation of China of China (NSFC, No. 51502325), NSFC-Guangdong Province Joint Fund (No. U1501246), M.S. Ma acknowledges the Youth Innovation Promotion Association of CAS, and G.Y. Chen acknowledges the UCAS Joint PhD Training Program of the international exchange.

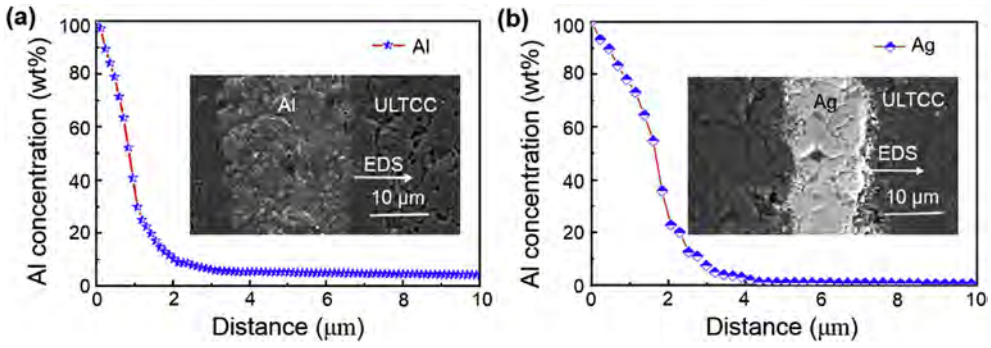

Fig. 9. (a) The concentration profiles of Al electrodes, (b) The concentration profiles of Ag electrodes.

References

[1] Y. Imanaka, Multilayered Low Temperature Co-fired Ceramics (LTCC) Technology, Springer publications, New York, 2007.
[2] M.T. Sebastian, R. Ubic, H. Jantunen, Microwave Materials and Applications, John Wiley & Sons Ltd, Finland, 2017, p. 2.
[3] K. Kim, J.M. Kim, J.M. Kim, G.C. Hwang, C.W. Baek, Y.K. Kim, LTCC substrate packaging for RF MEMS devices using LTCC substrate and BCB adhesive layer, J. Micromech. Microeng. 16 (2006) 150–156.
[4] M. Lahti, V. Lantto, Passive RF band-pass filters in an LTCC module made by fine-line thick-film pastes, J. Eur. Ceram. Soc. 21 (2001) 1997–2000.
[5] M.T. Sebastian, R. Ubic, H. Jantunen, Low-loss dielectric ceramic materials and their properties, Int. Mater. Rev. 60 (2015) 392–412.
[6] H. Yu, J. Liu, W. Zhang, S. Zhang, Ultra-low sintering temperature ceramics for LTCC applications: a review, J. Mater. Sci. Mater. Electron. 26 (2015) 9414–9423.
[7] J. Honkamo, H. Jantunen, G. Subodh, M.T. Sebastian, Tape casting and dielectric properties of $Zn_2Te_3O_8$-based ceramics with an ultra-low sintering temperature, Int. J. Appl. Ceram. Technol. 6 (2009) 531–536.
[8] K. Ju, H. Yu, L. Ye, G. Xu, Ultra-low temperature sintering and dielectric properties of SiO2-filled glass composites, J. Am. Ceram. Soc. 96 (2013) 3563–3568.
[9] M.T. Sebastian, H. Wang, H. Jantunen, Low temperature co-fired ceramics with ultra-low sintering temperatures: a review, Curr. Opin. Solid State Mater. Sci. 20 (2016) 151–170.
[10] G.H. Chen, L.J. Tang, J. Cheng, M.H. Jiang, Synthesis and characterization of CBS glass-ceramic composites for LTCC application, J. Alloy. Compd 478 (2009) 858–862.
[11] H. Zhu, H. Zhou, M. Liu, P. Wei, G. Ning, Low temperature sintering and properties of $CaO–B_2O_3–SiO_2$ system glass ceramics for LTCC applications, J. Alloy. Comp. 482 (2009) 272–275.
[12] X.F. Luo, L.C. Ren, W.T. Xie, L. Qian, Y.Z. Wang, Q.L. Sun, H.Q. Zhou, Microstructure, sintering and properties of $CaO–Al_2O_3–B_2O_3–SiO_2$ glass/Al_2O_3 composites with different CaO contents, J. Mater. Sci. Mater. Electron. 27 (2016) 5446–5451.
[13] C.J. Pei, G.G. Yao, Z.Y. Ren, Microwave dielectric properties of BaV_2O_6 ceramics with ultra-low sintering temperature, J. Ceram. Process. Res. 17 (2016) 681–684.
[14] H.T. Yu, K. Ju, K.M. Wang, A novel glass-ceramic with ultra-low sintering temperature for LTCC application, J. Am. Ceram. Soc. 97 (2014) 704–707.
[15] K. Ju, H. Yu, Y. Lin, Ultra-low temperature sintering and dielectric properties of SiO_2 -filled glass composites, J. Am. Ceram. Soc. 96 (2013) 3563–3568.
[16] M.S. Ma, Z.Q. Fu, Z.F. Liu, Y.X. Li, Fabrication and microwave dielectric properties of $CuO-B_2O_3-Li_2O$ glass-ceramic with ultra-low sintering temperature, Ceram. Int. 43 (2017) 292–295.
[17] S. Knickerbocker, M.R. Tuzzolo, S. Lawhorne, Sinterable β-spodumene glass-ceramic, J. Am. Ceram. Soc. 72 (1989) 1873–1879.
[18] S.H. Kweon, M.R. Joung, J.S. Kim, B.Y. Kim, S. Nahm, J.H. Paik, Y.S. Kim, T.H. Sung, Low temperature sintering and microwave dielectric properties of B_2O_3-added $LiAlSiO_4$ Ceramics, J. Am. Ceram. Soc. 94 (2011) 1995–1998.
[19] Z.F. Liu, Y.L. Wang, X.Y. Li, Combinatorial study of ceramic tape-casting slurries, ACS Comb. Sci. 14 (2012) 205–210.
[20] M.T. Sebastian, H. Jantunen, High Temperature Co-fired Ceramic (HTCC), Low Temperature Co-fired Ceramic (LTCC), and Ultralow Temperature Co-fired Ceramic (ULTCC) Materials, Microwave Materials and Applications vol. 1, John Wiley & Sons Ltd., 2017 (Chapter 8).
[21] J. Varghese, T. Siponkoski, M. Teirikangas, M.T. Sebastian, H. Jantunen, Structural, dielectric, and thermal properties of Pb free molybdate based ultralow temperature glass, ACS Sustain. Chem. Eng. 4 (2016) 3897–3904.
[22] B. Li, S. Wang, Y. Fang, Effect of Cr_2O_3 addition on crystallization, microstructure and properties of $Li_2O–Al_2O_3–SiO_2$ glass-ceramics, J. Alloy. Comp. 693 (2016) 9–15.
[23] M. Avrami, Kinetics of phase change: I. General theory, J. Chem. Phys. 7 (1939) 1103–1112.
[24] M. Avrami, Kinetics of phase change: II. Transformation-time relations for random distribution of nuclei, J. Chem. Phys. 8 (1940) 212–214.
[25] M. Avrami, Kinetics of phase change: III. Granulation, phase change and microstructure, J. Chem. Phys. 9 (1941) 177–184.
[26] C. Wu, J. Jean, Crystallization kinetics and dielectric properties of a low-fire $CaO–Al_2O_3–SiO_2$ glass + alumina system, J. Am. Ceram. Soc. 99 (2016) 2664–2671.
[27] S.M. Ohlberg, D.W. Strickler, Determination of percent crystallinity of partly devitrified glass by X-ray diffraction, J. Am. Ceram. Soc. 45 (1962) 170–171.
[28] M.P. Borom, A.M. Turkalo, R.H. Doremus, Strength and microstructure in lithium disilicate glass-ceramics, J. Am. Ceram. Soc. 58 (1975) 385–391.
[29] G. Xia, L. He, D. Yang, Preparation and characterization of $CaO-Al_2O_3-SiO_2$ glass/fused silica composites for LTCC application, J. Alloy. Comp. 513 (2012) 70–76.
[30] H.E. Kissinger, Variation of peak temperature with heating rate in differential thermal analysis, J. Res. Natl. Bur. Stnd. 57 (1956) 217–221.
[31] R. Freer, Diffusion in silicate minerals and glasses: a data digest and guide to the literature, Contrib. Mineral. Petrol. 76 (1981) 440–454.
[32] S. Ross, A.M. Welsch, H. Behrens, Lithium conductivity in glasses of $Li_2O-Al_2O_3-SiO_2$ system, Phys. Chem. Chem. Phys. 17 (2015) 465–474.
[33] J.H. Jean, C.R. Chang, Interfacial reaction kinetics between silver and ceramic-filled glass substrate, J. Am. Ceram. Soc. 87 (2004) 1287–1293.
[34] M.S. Ma, Z.F. Liu, F.Q. Zhang, Y.X. Li, Suppression of silver diffusion in borosilicate glass-based low-temperature cofired ceramics by copper oxide addition, J. Am. Ceram. Soc. 99 (2016) 2402–2407.